A portable gamma camera for the optimization of the patient dosimetry in radioiodine therapy of thyroid diseases

T. Bossis, M-A Verdier, L. Pinot, F. Bouvet, T. Beaumont, D. Broggio, S. Lamart
O. Caselles, S. Zerdoud, L. Ménard

***Abstract*—Molecular radiotherapy is an efficient treatment modality of benign and malign thyroid diseases. However, there is still a need to better assess the dose delivered to target tissues and organs-at-risk in order to optimize for each patient the activity to be administered according to the objectives of disease control (destruction of tumor residues or thyroid function) while maintaining the risk of toxicity at a justifiable level. In that context, our objective is to develop a high-resolution mobile gamma camera specifically designed to accurately measure the radiotracer biokinetics at the patient's bedside during treatment planning and therapeutic dose verification. A first feasibility prototype of the mobile camera with a 5×5 cm^2 field of view was developed for the treatment of benign and malign thyroid diseases with ^{131}I, leading to promising results. We are currently developing a new prototype for clinical use with extended field of view (10×10 cm^2). It consist of a 3D-printed parallel-hole tungsten collimator coupled to a 1 cm thick $CeBr_3$ scintillator, readout by an array of 6×6 mm^2 Silicon Photomultipliers. Preliminary results show a energy resolution of 8% and a FWHM spatial resolution around 1 mm at 356 keV. A detailed description of the camera optimization (collimator and shielding design, intrinsic spatial performance, counting rate capabilities) will be presented.**

I. Introduction

Targeted radionuclide therapy is one of the most widespread treatment modality for benign and malignant thyroid diseases. However, the personalization of treatments and the precise dosimetry it implies are not yet solidly established methods in the medical world. Indeed, as each patient has his own biokinetics, it is important to adapt the absorbed dose for each case in order to maximize the therapeutic effects on the target tissues while minimizing the toxicity for organs-at-risk. At present, the measurement of the absorbed dose by the patient is performed by measuring the activity of a sample obtained by biopsy or by external counting probes. These methods do not take into account the heterogeneous spatial distribution of radioactivity in the dose evaluation. Therefore, imaging methods are preferred for quantification of the radiotracer biokinetics. However, planar or SPECT cameras are not optimized for imaging with high energy gamma rays and high photon fluences. Moreover, the acquisition of these images must be repeated at specific times before and after treatment administration, which poses the problem of the availability of the imaging devices. In order to overcome these shortcomings, our objective is to develop a portable high-resolution gamma camera specifically optimized for dose quantification at the patient's bedside during the treatment of malign and benign thyroid diseases with ^{131}I. It will be used to measure the biokinetics of ^{131}I in the thyroid, tumor remnants, metastatic lymph nodes or salivary glands during both treatment planning and therapeutic dose verification. A first prototype of gamma camera with a 5×5 cm^2 field of view (FoV) has been previously developed [1]. Thanks to very its very good intrinsic energy and spatial resolutions and compactness, the camera is able to quantify homogeneous and heterogeneous activity distributions (such as nodules) on 3D thyroid phantoms with an error less than 10% and a very simple quantification protocol. Based on these very promising results, we are currently developing a fully operational clinical version of the mobile gamma camera with a 10×10 cm^2 FoV suited to the size of the thyroid, millimetric spatial performance and increased counting capabilities (200 kcps).

T. Bossis, L. Pinot and F. Bouvet are with Université Paris-Saclay, CNRS/IN2P3, IJCLab, ORSAY, France

M-A Verdier and L. Ménard are with Université Paris-Saclay, CNRS/IN2P3, IJCLab, ORSAY, France and Université de Paris, IJCLab, ORSAY, France

T. Beaumont, D. Broggio and S. Lamart are with IRSN, LEDI, FONTENAY-AUX-ROSES, France

O. Caselles and S. Zerdoud are with IUCTO, ICR, TOULOUSE, France

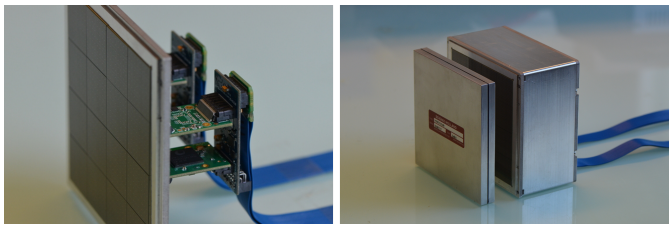

Figure 1: *Photo-detection system of the clinical prototype of the mobile camera (left) and its $CeBr_3$ scintillator and enclosure (right).*

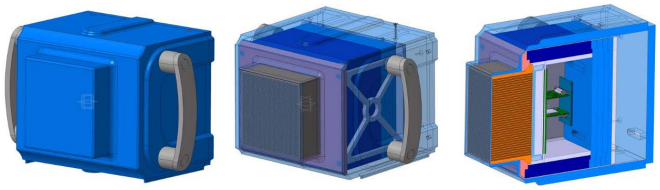

Figure 2: *3D view of the fully integrated new clinical prototype*

II. Design of the gamma camera

The mobile gamma camera is composed of a tungsten parallel hole collimator printed by Selective Laser Melting (SLM) technology. The collimator is coupled to a 10×10 cm^2 and 1 cm thick monolithic $CeBr_3$ scintillator with reflective optical coatings. The photodetection system consists of 4×4 Hamamatsu S13361-6050 arrays of 4×4 silicon photomultipliers (SiPMs) (fig. 1). The pixels have an effective sensitive area of 6×6 mm^2 and a micro-cell size of 50×50 μm^2 (fig. 1). The signals produced by the SiPMs are shaped and digitized by a commercial front-end electronics manufactured by the PETSys company. It is composed of four TOFPET 2B ASIC with 64 analog reading channels. The whole camera is protected from the radioactive background by a combination of lead and tungsten shielding (fig. 2). The camera will be held by a mechanical positioning system in order to bring it close to the neck, at different angles of incidence.

III. Collimator and shielding optimization

The features of the parallel hole collimator were determined using GATE Monte-Carlo simulations in order to obtain the best compromise between sensitivity, spatial resolution and septal penetration by high-energy gamma rays. Several hexagonal shaped collimator designs were investigated with a ^{131}I line source (fig. 3). An accurate characterization of the energy and spatial distributions of scattered and penetration events was performed. Based on simulation results and interpolation methods, the design of two interchangeable collimators, with a septal penetration of 7.5%, were chosen. The first one is able to achieved a spatial resolution of 3 mm FWHM and a sensitivity of 32 cps/MBq at 5 cm (1.8 mm diameter hole, 0.84 mm septal thickness and 58.7 mm length). This configuration is dedicated to high resolution imaging for the assessment of absorbed dose in

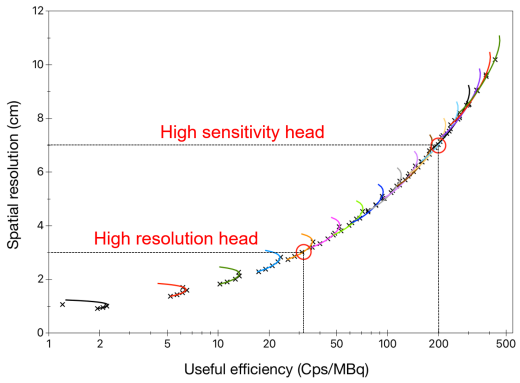

Figure 3: *Useful efficiency as a function of the spatial resolution for different collimators with effective septa penetration of 7.5%.*

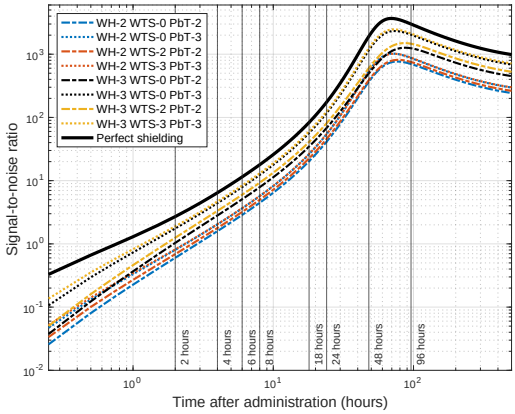

Figure 4: *Signal (thyroid)-to-noise (other organs) ratio as a function of the shielding and the time after ^{131}I administration. Data obtained for a low uptake in the thyroid (15% at 24h).*

the thyroid or tumor remnants during post-treatment monitoring of thyroid cancers. The second configuration was chosen to achieve high sensitivity during treatment planning of hyperthyroidism or imaging of metastatic lymph nodes or salivary glands during post-treatment verification of thyroid cancers, that are characterized by moderate levels of activity. Its geometric features (4.02 mm diameter hole, 1.69 mm septal thickness and 54.4 mm length) allow to reach a sensitivity of 200 cps/MBq and a spatial resolution of 7 mm FWHM at 5 cm. In order to determine the best shielding compromise in terms of noise reduction, space requirement and weight of the camera, a more realistic clinical context was simulated using the XCAT voxelized phantoms. Both background and thyroid activity distributions encountered during thyroid treatment were simulated in each organ at different time after ^{131}I ingestion by using the Leggett biokinetic model of Iodine [2]. The design of the complete camera was fully modeled and its intrinsic performances were set according to the experimental results achieved with the feasibility prototype. It was shown that a 3 cm thick tungsten shielding on the front of the camera and a 3 cm thick lead shielding around the rest of the camera except for the top (2 cm) provided near perfect shielding and a signal-to-noise ratio of 8 for early imaging 6 hours after ^{131}I administration (fig. 4).

IV. Intrinsic performances

The spatial and energy performance were evaluated by using a ^{133}Ba source collimated by a tungsten collimator with a 0.5 m and 4 mm diameter hole, respectively. Thermal noise events (11 kCps for the operative bias and individual trigger threshold used) are completely suppressed by an internal hardware trigger (10ns coincidence window) which operates between two regions of the photodetector

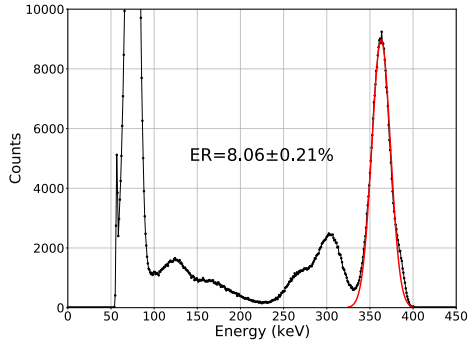

Figure 5: *^{133}Ba energy spectrum measured at optimal SiPMs and electronics parameters.*

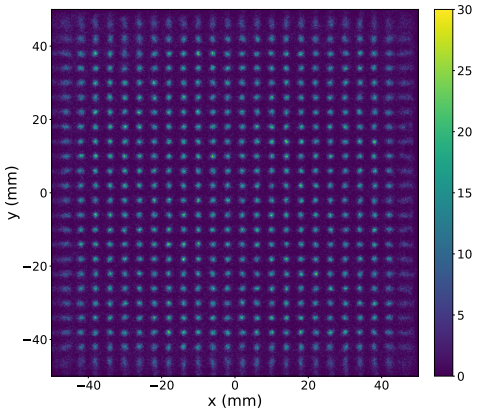

Figure 6: *Reconstructed ^{133}Ba scan of the field of view with a step of 4 mm.*

defined as a checkerboard where each square corresponds to a 4×4 SiPM array. The non uniformity of the photodetector light response was evaluated and corrected by irradiating the field of view with a pulsed LED source. The relative standard deviation of the light responses over the 256 pixels before and after correction are 12.8% and 0.96%, respectively. The average energy resolution at 356 keV is 8.06±0.21% FWHM in the CFOV (fig. 5). The spatial response of the camera was investigated by scanning the FoV with the collimated source and a 1 mm pitch in order to measure the 2D light response function for each pixel. Events are reconstructed from a non-linear least square minimization between its charge distribution and the light distributions interpolated from the light response. The average spatial resolution in the center of the field of view is 1.18±0.11 mm FWHM with a mean positioning bias of 0.10±0.06 mm (fig. 6). The system has a maximum counting rate of 40 kHz (transfer of the 256 channels for each detected event).

V. Conclusion

Our intrinsic performances evaluation shows that the combination of the PETSys electronics readout and the S13361-6050 SiPMs array allows to reach the initial objectives in terms of performances (intrinsic spatial resolution of the order of 1 mm and an energy resolution around 8% at 356 keV) and clinical requirements (field of view and compactness). Image reconstruction algorithms are still being optimized to achieve fast and accurate events positioning on the edges of the FoV, for instance with artificial neural networks. The counting capability will also be increased up to 200 kcps by using an optical fiber transmission line, opening the door to early imaging just after treatment administration. The overall performances of the fully integrated 10×10 cm^2 field of view mobile camera will be presented at the conference.

References

[1] C. Trigila, Phys Med Biol, 2022, 10.1088/1361-6560/ac4c31.
[2] R. W. Leggett, Radiat Res, vol. 174, no. 4, pp. 496–516, Oct. 2010.